Geochemical Perspectives Letters

Orbitally forced sphalerite growth in the Upper Mississippi Valley District

M. Li, H. L. Barnes

Supplementary Information

The Supplementary Information includes:

- Materials and Methods
- Supplementary Text
- Tables S-1 and S-2
- Figures S-1 to S-12
- Supplementary Information References

Materials and Methods

The timing of the sphalerite deposition in the Upper Mississippi Valley District (UMVD, Fig. S-1) has been dated at 270 ± 4 Ma from Rb-Sr isochrons of three sphalerite bands (Brannon *et al.*, 1992), matching with a contemporaneous, genetically-related igneous activity in the Illinois Basin dated with average Ar-Ar age of 271.3 ± 0.6 Ma (Rowan and Goldhaber, 1996). The sample analyzed in the main text is Sample 58 of McLimans *et al.* (1980) (Fig. 1 as in main text). The sphalerite stratigraphy in the UMVD has been divided into three stages: A (early), B (middle), and C (late) and the studied Sample 58 represents the entire period of sphalerite deposition.

Rock colors, including grayscale, can be interpreted as qualitative measurements of climate conditions for marine and terrestrial sediments (Li *et al.*, 2019b). The darkness of the banding correlates with the iron content of the sphalerite. Comparison between relative absorbance of transmitted light and relative FeS intensity of a sphalerite sample in the Edgerton orebody (Fig. S-2) confirmed the color of the sphalerite is related to the FeS content (McLimans *et al.*, 1980). However, that function does not directly define the periodicities in the data. For this study, sphalerite samples were first cut and polished. Then scanning of the sphalerite digitalized the color data of the samples in the RGB (red-green-blue) format. We use a time series software *Acycle* 1.0 (Li *et al.*, 2019a) to transform the RGB image in the grayscale color system. This tool converts RGB values to grayscale values by forming a weighted sum of the R, G, and B components using MatLab's rgb2gray algorithm (https://www.mathworks.com/help/matlab/ref/rgb2gray.html): grayscale value = 0.2989 * R + 0.5870 * G + 0.1140 * B. Then the grayscale profile is extracted using the "Image Profile" function in *Acycle* (Li *et al.*, 2019a). To test the reliability of the "Image Profile" function in *Acycle*, we also extract the grayscale profile using another software *ImageJ* package (Abràmoff *et al.*, 2004).

The identification of Milankovitch cycles of sphalerite deposition follows typical procedures (Li *et al.*, 2019a). The rock color series are detrended using *Acycle*'s "Detrending" function subtracting a linear trend (Li *et al.*, 2019a) so that the mean of the data is zero. The linear trend can either be a long-term climate signal or a secular change in the ore solution. The resulting data (with a zero mean) was analysed using Fourier transform methods to identify any significant periodicities (termed power spectra, which are a series of numbers giving the spectral amplitude as a function of frequency, in this case inverse distance or mm^{-1}). Here both

2π multi-taper (MTM) power spectrum and periodogram are calculated using "*Spectral Analysis*" function of *Acycle* for the grayscale series to search for dominated wavelengths of the series related to potential astronomical cycles. The significance of the MTM power spectrum of the grayscale series is shown with robust red-noise models (Mann and Lees, 1996), which is estimated using the "*Spectral Analysis*" function of *Acycle*. Gaussian bandpass filter (Kodama and Hinnov, 2015) was applied to isolate potential astronomical parameters using "Filtering" function in *Acycle* (Li *et al*., 2019a). To relate the spacing variations to time variations (and hence to Milankovitch frequencies) one must know the deposition rate of the sphalerite growth. A given deposition rate would convert the grayscale values *vs*. distance into grayscale values *vs.* time by the simple relation: time = distance / deposition rate.

To unravel the actual value of deposition rate, the COCO method is used, which evaluates the correlation coefficient (ρ) between power spectra of a proxy time series and an astronomical target, converting the proxy data from depth to time for a range of test sedimentation rate (Li *et al*., 2018). The significance of the deposition rates is evaluated by comparison to values expected from a chance correlation using Monte Carlo methods. 2000 random spectral values with random frequencies and random amplitudes were generated to compare a random (chance) correlation to the actual power spectrum of the sphalerite time series for a given deposition rate. High COCOs with high significance would prove the direct effect of Milankovitch climate variations on the formation of the sphalerite bands and thus on the formation of Mississippi Valley-Type (MVT) ore deposits.

In comparison, the TimeOpt method simultaneously estimates the eccentricity-related amplitude modulation of the precession band (measured as $r^2_{envelope}$) and the concentration of spectral power at precession and eccentricity frequencies (measured as r^2_{power}) for a range of test sedimentation rate (Meyers, 2015). The final measure of fit (r^2_{opt}) is defined as $r^2_{opt} = r^2_{envelope} * r^2_{power}$. The r^2_{opt} values range from 0 to 1, and 1 is a perfect fit to the models. Test deposition rates range from 0.005 μm/a to 0.5 μm/a with a step of 0.001 μm/a.

Based on the astronomical theory that described the gravitational effects of the Solar system, the accurate Milankovitch cycles can be calculated (Table S-1). The calculated Milankovitch cycles are currently 405 kyr, 125 kyr and 95 kyr eccentricity cycles, 55 kyr and 41 kyr obliquity cycles, 24 kyr and 19 kyr precession cycles (Laskar *et al*., 2004). Due to the change in the Earth-Moon distance through tidal friction, the obliquity and precession cycles have been smaller than today's (Berger *et al*., 1989). At 270 Ma, periods of Milankovitch cycles were 413 kyr, 123 kyr, 95 kyr, 44.3 kyr, 35.1 kyr, 21.0 kyr, and 17.6 kyr (Berger *et al*., 1989), and these values are used in both COCO and TimeOpt estimation.

Supplementary Text

Analyses of the time series

In the main text, we show a time series analysis result of *Acycle*-generated grayscale profile of Sample 58 from West Hayden orebody. Below are similar results using *ImageJ* software-generated grayscale profile of Sample 58 and *Acycle*-generated grayscale profiles of samples collected from Hendrickson and Edgerton (Fig. 1 in the main text).

West Hayden Orebody (*ImageJ*-generated grayscale profile)

Power spectral analysis of *ImageJ* software-generated grayscale data (Figs. S-3 and S-4) indicates the significant frequency peaks corresponding to 35 mm, 10-8 mm, 1.78 mm, and 1.23 mm cycles (Fig. S-5). Statistical analysis using both COCO and TimeOpt methods give similar results (Fig. S-6). The COCO results suggest the correlation coefficient (ρ) value reaches the higher peak at the depositional rate of 0.300 μm/a at which the null hypothesis (H_0, no orbital forcing) significance level is 0.25 %. There is a peak at 0.08 μm/a but the ρ is a much lower than that at 0.300 μm/a. In comparison, the TimeOpt analysis indicates the highest $r^2_{envelope}$ peak occurs at 0.268 μm/a, the highest peak of r^2_{power} at 0.082 μm/a, and the highest r^2_{opt} peak at 0.268 μm/a. A combination of above analyses suggests the optimal depositional rate of the studied sphalerite sample is probably at 0.268-0.300 μm/a. Therefore, the null hypothesis of no orbital forcing can be rejected at a confidence level of 99.75 % and the dominated 35 mm cycles are 116-130 kyr (probably short eccentricity) cycles, and the 8.76 mm and 1.78-1.23 mm cycles are probably 29-33 kyr (obliquity) and 6-4 kyr (sub-Milankovitch) cycles.

Hendrickson Orebody

Power spectral analysis of *Acycle*-generated grayscale data (Fig. S-7) of sample from the Hendrickson orebody (Figure 1, main text) indicates frequency peaks corresponding to 45 mm, 14.5-11.2 mm, 6-3.8 mm, and 1.2 mm cycles (Fig. S-8). Statistical analysis using both COCO and TimeOpt methods give similar results (Fig. S-9). The COCO results suggest the correlation coefficient (ρ) value reaches the higher peak at the depositional rate of 0.35 μm/a at which the null hypothesis (H_0, no orbital forcing) significance level is 0.55 %. There is a peak at 0.11 μm/a but the ρ is a much lower than that at 0.35 μm/a. In comparison, the TimeOpt analysis

indicates the highest $r^2_{envelope}$ peak occurs at 0.35 μm/a, the highest peak of r^2_{power} at 0.12 μm/a, and the highest r^2_{opt} peak at 0.35 μm/a. A combination of above analyses suggests the optimal depositional rate of the sphalerite sample from the Hendrickson orebody is probably at 0.35 μm/a. Therefore, the null hypothesis of no orbital forcing can be rejected at a confidence level of 99.45 % and the dominated 45 mm cycles are 129 kyr (probably short eccentricity) cycles, and the 14.5-11.2 mm, 6 mm, 3.8 mm, and 1.2 mm cycles are probably 41-32 kyr (obliquity), 17.1 kyr (precession), 11 kyr, and 3.4 kyr (sub-Milankovitch) cycles.

Edgerton Orebody

Power spectral analysis of *Acycle*-generated grayscale data (Fig. S-10) of sample from the Edgerton orebody (Figure 1, main text) indicates the significant frequency peaks corresponding to 13.8 mm and 1.2 mm and other peaks at 25.6 mm, 9.4-6.9 mm, and 3.5 mm cycles (Fig. S-11). Statistical analysis of this shorter grayscale series using both COCO and TimeOpt methods give slightly different results (Fig. S-12). The COCO results suggest the correlation coefficient (ρ) value reaches the higher peak at the depositional rate of 0.21 μm/a at which the null hypothesis (H_0, no orbital forcing) significance level is 0.05 %. There is a peak at 0.07 μm/a but the ρ is a much lower than that at 0.21 μm/a. In comparison, the TimeOpt analysis indicates the highest $r^2_{envelope}$ peak occurs at 0.27 μm/a, the highest peak of r^2_{power} at ~0.07 μm/a, and the highest r^2_{opt} peak at 0.27 μm/a. A combination of above analyses suggests the optimal depositional rate of the sphalerite sample from the Hendrickson orebody is probably at 0.21-0.27 μm/a. Therefore, the null hypothesis of no orbital forcing can be rejected at a confidence level of 99.45 % and the significant 13.8 mm and 1.2 mm cycles are 66-51 kyr and 5.7-4 kyr cycles, respectively. And the high amplitude cycles of 25.6 mm, 9.4-6.9 mm, 3.5 mm cycles are probably 122-95 kyr (short eccentricity), 45-26 kyr (obliquity), and 17-13 kyr (precession?) cycles.

Deposition rates

There is a peak deposition rate at 0.08 μm/a for the sample from the West Hayden Site (Figs. 4 and S-6). There are also comparable peaks at 0.11 μm/a at the Hendrickson Site (Fig. S-9) and 0.07 μm/a at Edgerton Site (Fig. S-12). Take the West Hayden sample as an example, if the deposition rate at 0.08 μm/a instead of 0.27 μm/a is used, then the dominant periodicities are 400 kyr, 117.5-95 kyr, 21.9-12.5 kyr, and 7.3 kyr. These compare with the Permian Milankovitch cycles listed above. However, there are three lines of evidence that support the 0.27 μm/a rather than 0.08 μm/a deposition rate in this case. First, as shown in Figure 4a, the correlation coefficient at 0.27 μm/a is much higher than that at 0.08 μm/a suggesting that the deposition rate at 0.27 μm/a has a much better fit than that at 0.08 μm/a. Second, the TimeOpt analysis indicates the highest $r^2_{envelope}$ peak occurs at 0.27-0.36 μm/a and no peak at 0.08 μm/a, and the highest r^2_{opt} peak at 0.29-0.36 μm/a and very low peak at 0.08 μm/a. A combination of information from precession amplitude and power spectra suggests the optimal depositional rate of the studied sphalerite sample is probably 0.27 μm/a. Third, from radiometric dating and modeling of diffusion and heat and flow rates, apparently sphalerite was deposited for about 0.25 My in layers up to 5 cm maximum thickness at a rate of about 0.2 μm/a (Barnes, 2015), this conclusion is in agreement with an independent estimation of 0.212 Myr in duration (Rowan and Goldhaber, 1996). In sum, the deposition rates of these sites are 0.27 μm/a at West Hayden, 0.35 μm/a at Hendrickson, and 0.21-0.27 μm/a at Edgerton.

The depositional rate of 1-7 μm/a by Roedder (1968) is one order of magnitude higher than our result derived from statistical methods. The varves recognized by Roedder (1968) are probably decadal, not annual, varves.

Variable deposition rate *vs*. constant deposition rate

COCO analysis of synthetic series and real proxy data with constant and variable sedimentation rates suggests the COCO analysis result is insensitive to sedimentation rate changes (Li *et al*., 2018). The COCO aided with the sliding procedure enables the evolutionary COCO analysis, which is designed for detecting variable sedimentation rate. For example, COCO analysis of a synthetic series (#2 in Li *et al*., 2018; with modeled 4 and 6 cm/kyr sedimentation rates) shows strong peaks at 4 and 6 cm/kyr. COCO analysis of Fe series at Ocean Drilling Program (ODP) site 1262 indicates multiple peaks at 1.21, 0.98, and 0.73 cm/kyr, all of which are confirmed by higher resolution eCOCO analysis result (Li *et al*., 2018). In comparison, COCO analysis of the Triassic Newark depth rank series shows a single broad peak at 15 cm/kyr, this is also confirmed by eCOCO result that suggests the sedimentation rates throughout the series are generally stable at ~15 cm/kyr (Li *et al*., 2018). eCOCO analysis does not apply to the grayscale series in this study, because it requires the time series data long enough to allow for the sliding window procedure and each sliding window can cover sufficient data to correctly recognize the optimal deposition rate. However, the single broad peak at 0.27 μm/a from COCO analysis of the sphalerite samples from West Hayden (Fig. 4a, main text) suggests that the actual deposition rate varies a little bit and centers at 0.27 μm/a. The same argument holds for other COCO results for other samples. Therefore, the non-constant deposition rate won't affect the conclusion of this paper.

Precipitation rates

Lasaga (1984) has precipitation rates for several silicates likely to be hydrothermally deposited. Recalculating his data from Table 5 shows that our 0.2 μm/a is roughly in the middle of his range from 0.003 to 600 μm/a (Table S-2). Our rate is also comparable to the precipitation rate of the calcite (~0.6-1 μm/a) that precipitated from calcite-supersaturated groundwater over the past 200 kyr from the Devil Hole, Nevada (Moseley *et al*., 2016).

Hydrothermal Modeling

The Illinois Basin in the Permian provided the Mississippi Valley Type deposits (MVTD) ore solutions after deep basin heating apparently by both igneous and mantle sources. Currently or in the past, analogous basins might generate such deposits by providing outflow of organic-rich solutions at depths of about 5 km with >100 ppm Zn, 150 - 250 °C for flow persistence >~0.5 Myr (Barnes, 2015). In the United States, of 17 basins examined for potential thermal or petroleum production, only 3, the Anadarko, Uinta, and Green River Basins are now warm enough (Anderson, 2013). Data from 49 basins globally that may be MVTD-productive have been compiled by Nelson and Kibler (2003). Searches of older basins with the pertinent characteristics could be bases for an exploration program.

Supplementary Tables

Table S-1 Astronomical periodicities in thousand years: at present (from Laskar *et al.*, 2004) versus Permian time (270 million years ago, from Berger *et al.*, 1989).

From banding in sphalerite	From astronomical solutions					
	Eccentricity		Obliquity		Precession	
	At present	Permian	At present	Permian	At present	Permian
	405	413				
	125	123				
118.5	95	95				
			55	44.3		
34.8			41	35.1		
					24	21.0
14					19	17.6

Table S-2 Precipitation rates for several silicates likely to be hydrothermally deposited (from Lasaga, 1984).

Mineral	Precipitation rates (μm/a)
Forsterite	600
K-feldspar	520
Albite	80
Enstatite	8.8
Diopside	6
Nepheline	0.21
Anorthite	0.11
Quartz	0.034
Muscovite	0.003

Supplementary Figures

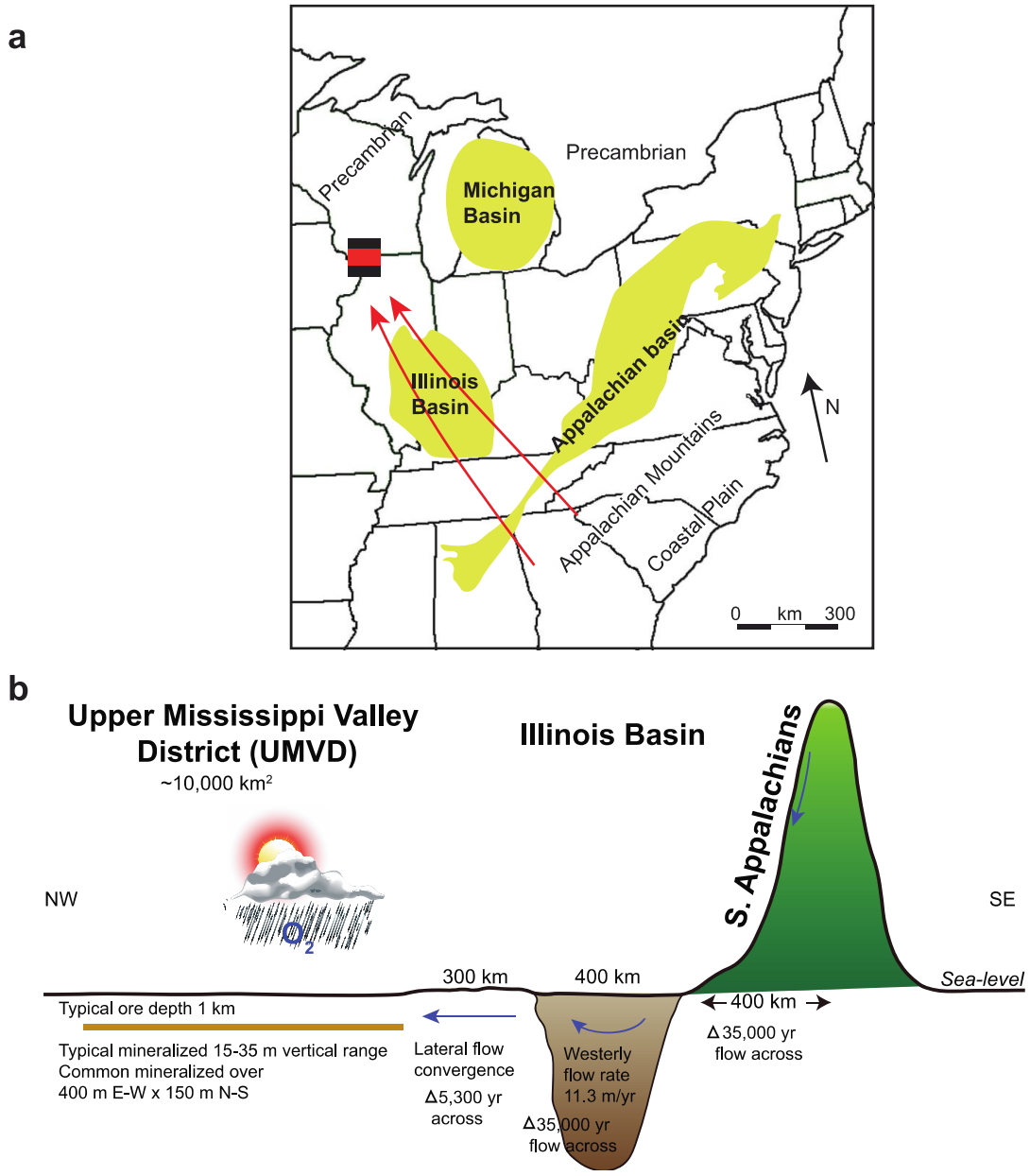

Figure S-1 Schematic model of water flow from the elevated South Appalachians through the Illinois Basin to the Upper Mississippi Valley District (UMVD). Both (a) and (b) are based on Bethke (1986) and summary in Barnes (2015).

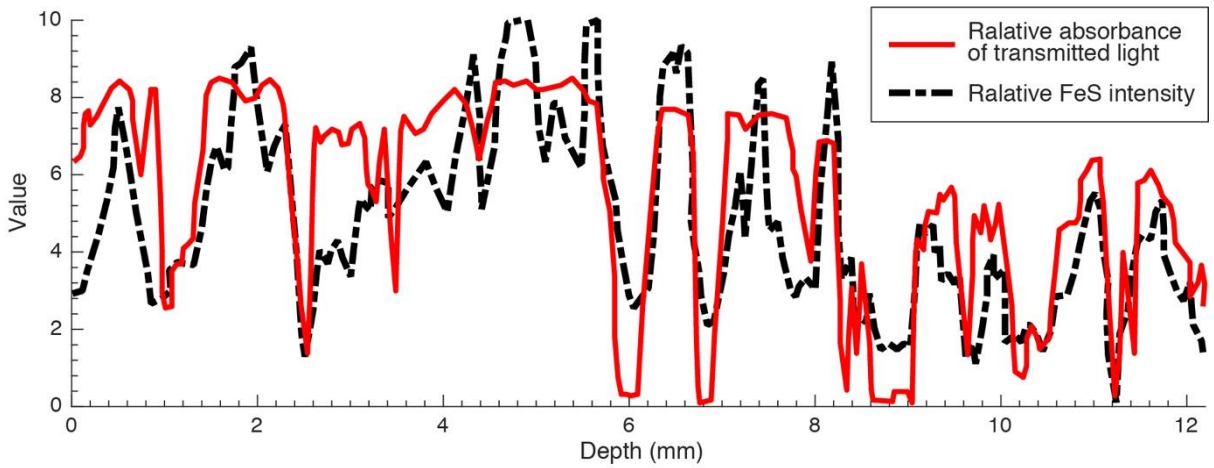

Figure S-2 Relative absorbance of transmitted light (solid red line) versus relative FeS intensity (dashed black line) for a portion of the sample in the Edgerton orebody (McLimans *et al.*, 1980). Color of sphalerite is nearly black at maximum absorption (10) and nearly white at minimum absorption (0).

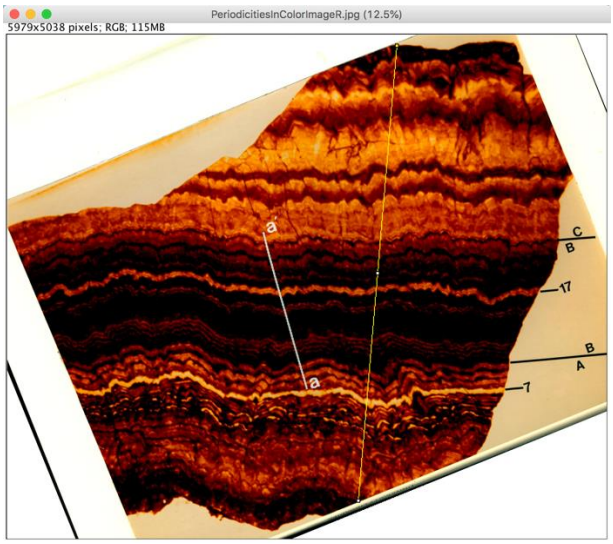

Figure S-3 Image of sphalerite sample in *ImageJ* software from the West Hyden Orebody. Colored photographs are shown with three growth stages of A (early), B (middle), and C (late) following McLimans *et al.* (1980). The rock colour grayscale profile was measured along the traverse (yellow line). Length of the line of a-a' is 20 mm.

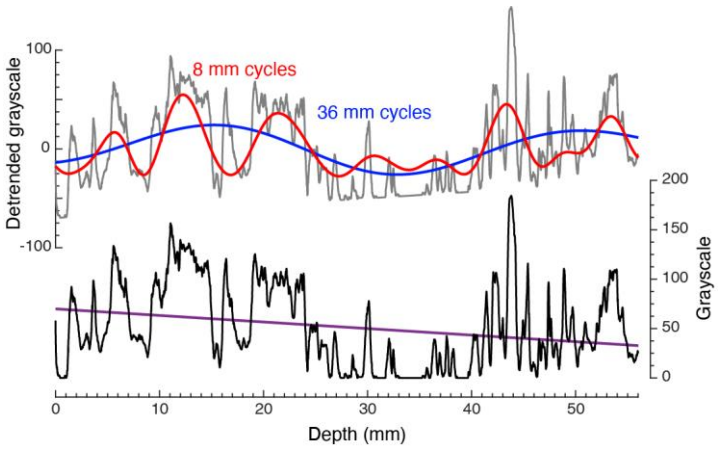

Figure S-4 Grayscale of the sphalerite (black) and its linear trend (purple). Detrended data (gray) are shown with its 35 mm (blue) and 8 mm (red) Gauss bandpass-filtered cycles (passband: 0.028 ± 0.008 and 0.12 ± 0.08 cycles/mm, respectively).

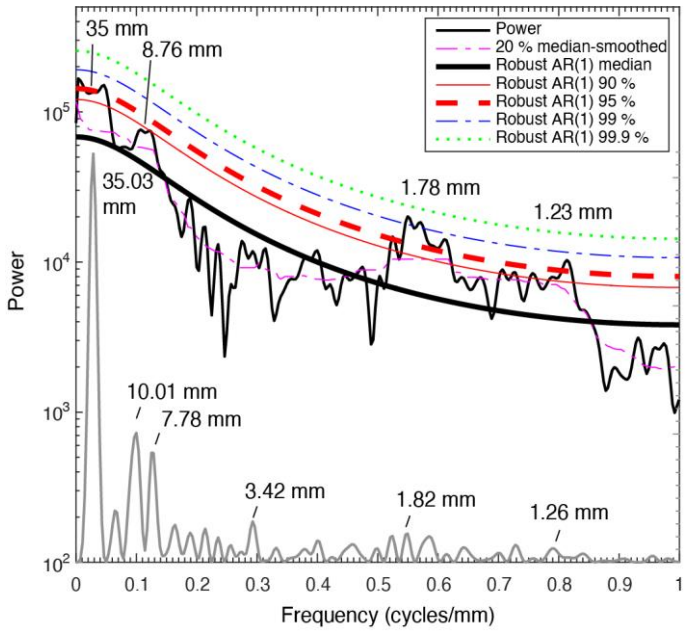

Figure S-5 2π MTM power spectrum (thin black) and periodogram (gray) of the grayscale series shown with robust red-noise models. The red-noise fit to the spectrum is based on the best fit to the log power of the 20 % median-smoothed spectrum (dashed pink). The 90 % (solid red), 95 % (dashed red), 99 % (blue dashed line), and 99.9 % (dot green) confidence limits are shown. Cycle wavelengths are also marked.

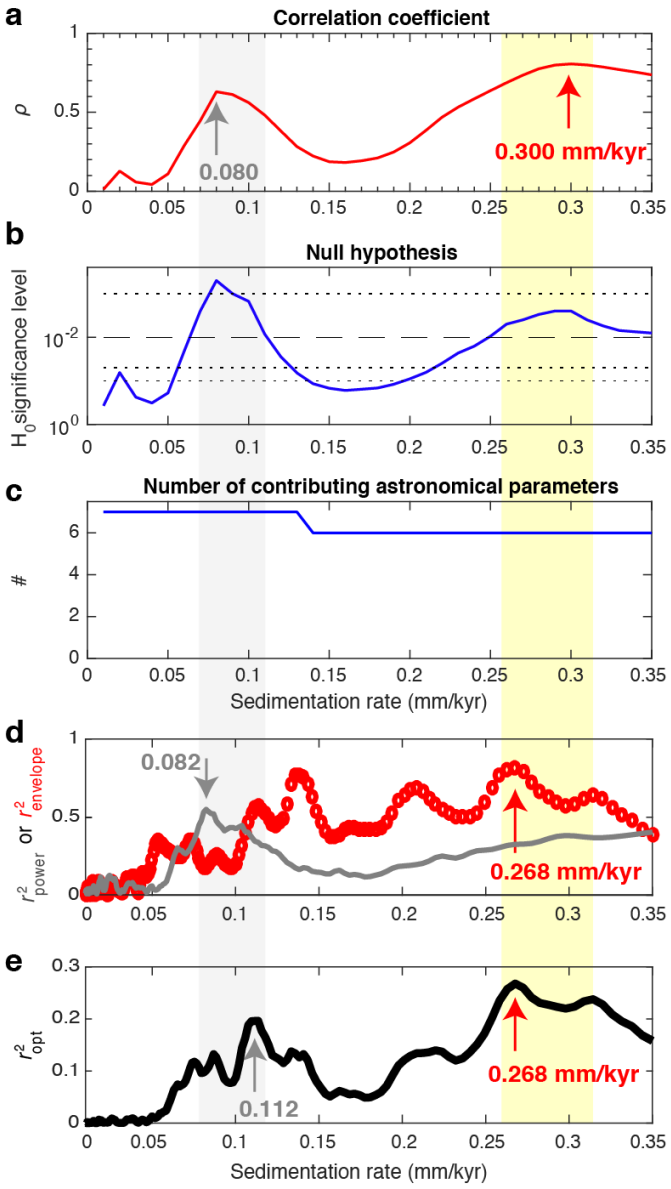

Figure S-6 Sphalerite deposition rate. (**a**) The COCO analysis shows optimal deposition rate at 0.30 µm/a. (**b**) Null hypothesis testing of the data series indicates that 0.08 µm/a and 0.30 µm/a deposition rate have significance levels less than 1 %. Significance levels are estimated using Monte Carlo simulations of 2000 iterations. (**c**) Number of contributing astronomical parameters in the test deposition rate ranging from 0.001 to 0.35 with a step of 0.001 µm/a. (**d**) Squared correlation coefficient for the amplitude envelope fit ($r^2_{envelope}$) and the spectral power fit (r^2_{power}) at test deposition rate ranging from 0.001 to 0.35 µm/a with 200 steps. (**e**) Combined envelope and spectral power fit (r^2_{opt}) at test deposition rate indicating the optimal deposition rate of 0.268 µm/a.

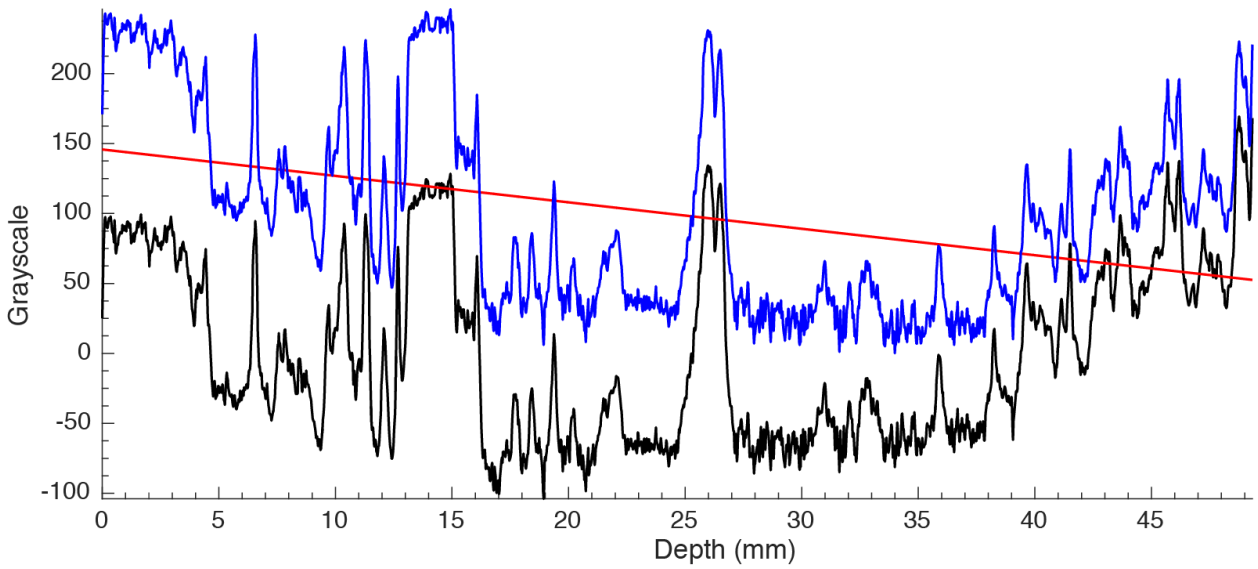

Figure S-7 Grayscale of the sphalerite from Hendrickson orebody (blue) and its linear trend (red) shown with detrended data (black).

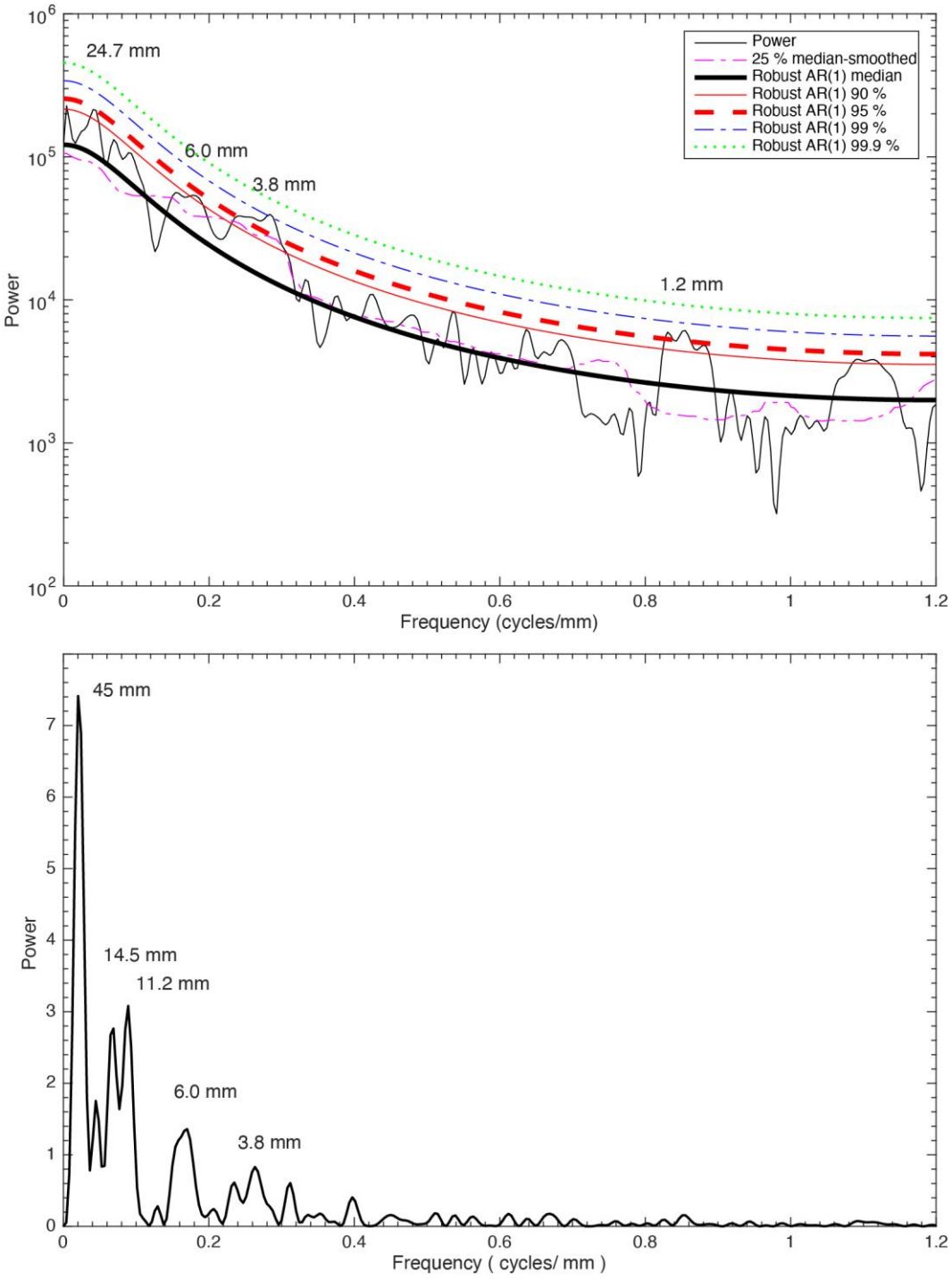

Figure S-8 2π MTM power spectrum (upper panel) and periodogram (lower panel) of the grayscale series of the sphalerite sample from Hendrickson orebody (Fig. 1, main text) shown with robust red-noise models. The red-noise fit to the spectrum is based on the best fit to the log power of the 25 % median-smoothed spectrum (dashed pink). The 90 % (solid red), 95 % (dashed red), 99 % (blue dashed line), and 99.9 % (dot green) confidence limits are shown. Cycle wavelengths are also marked.

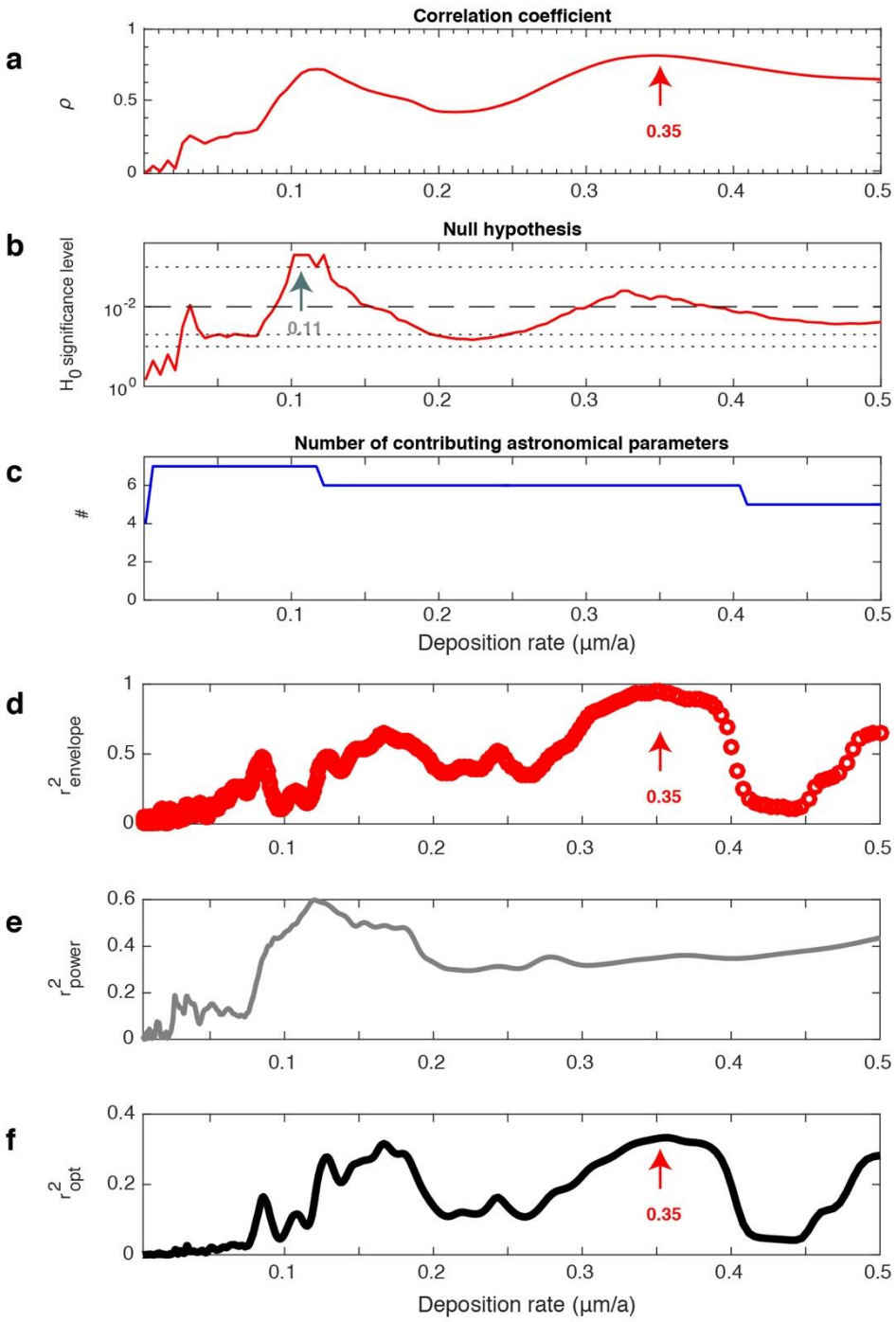

Figure S-9 Sphalerite deposition rate. (**a**) The COCO analysis shows optimal deposition rate at 0.35 µm/a. (**b**) Null hypothesis testing of the data series indicates that 0.11 µm/a and 0.33 µm/a deposition rate have significance levels less than 1 %. (**c**) Number of contributing astronomical parameters in the test deposition rate ranging from 0.005 to 0.5 with a step of 0.001 µm/a. (**d**) Squared correlation coefficient for the amplitude envelope fit ($r^2_{envelope}$) and (**e**) the spectral power fit (r^2_{power}). (**f**) Combined envelope and spectral power fit (r^2_{opt}) at test deposition rate indicating the optimal deposition rate of 0.35 µm/a.

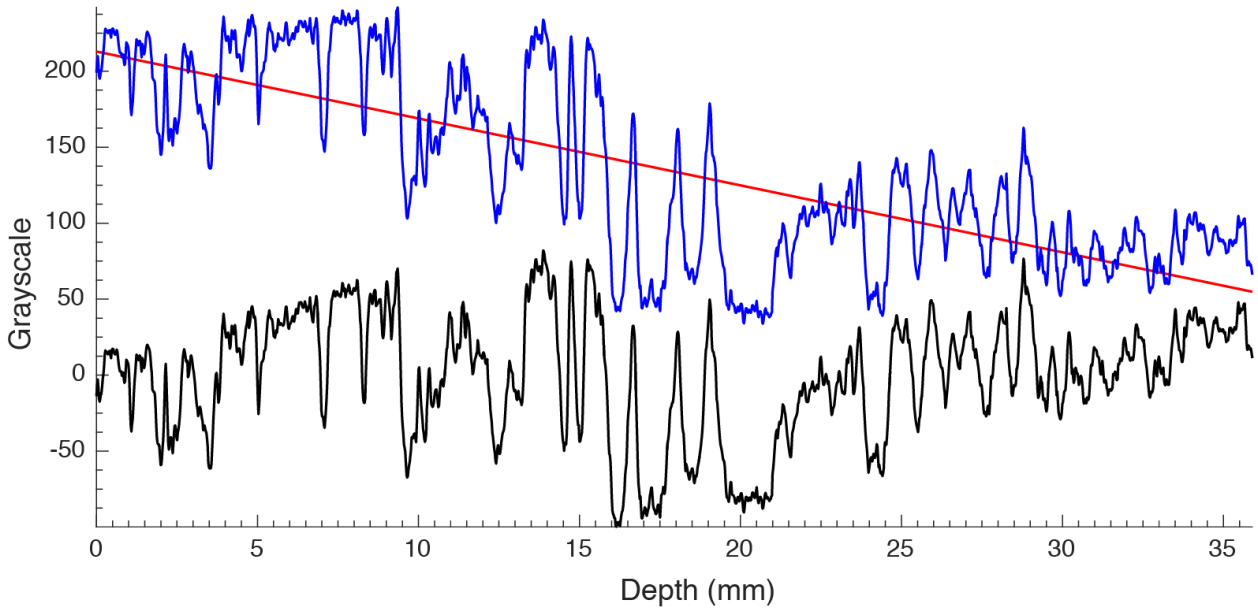

Figure S-10 Grayscale of the sphalerite from Edgerton orebody (blue) and its linear trend (red) shown with detrended data (black).

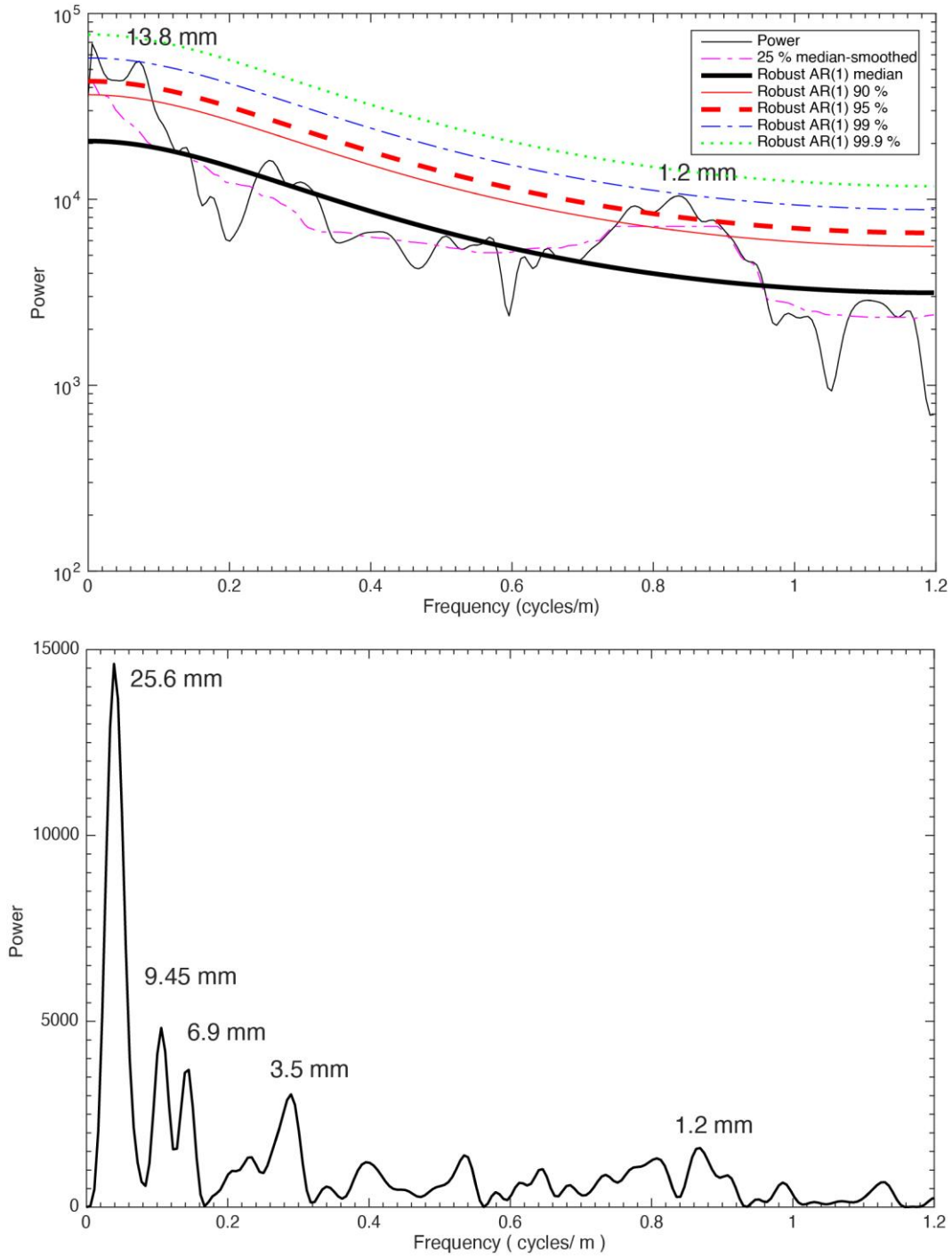

Figure S-11 2π MTM power spectrum (upper panel) and periodogram (lower panel) of the grayscale series of the sphalerite sample from Edgerton orebody (Fig. 1, main text) shown with robust red-noise models. The red-noise fit to the spectrum is based on the best fit to the log power of the 25 % median-smoothed spectrum (dashed pink). The 90 % (solid red), 95 % (dashed red), 99 % (blue dashed line), and 99.9 % (dot green) confidence limits are shown. Cycle wavelengths are also marked.

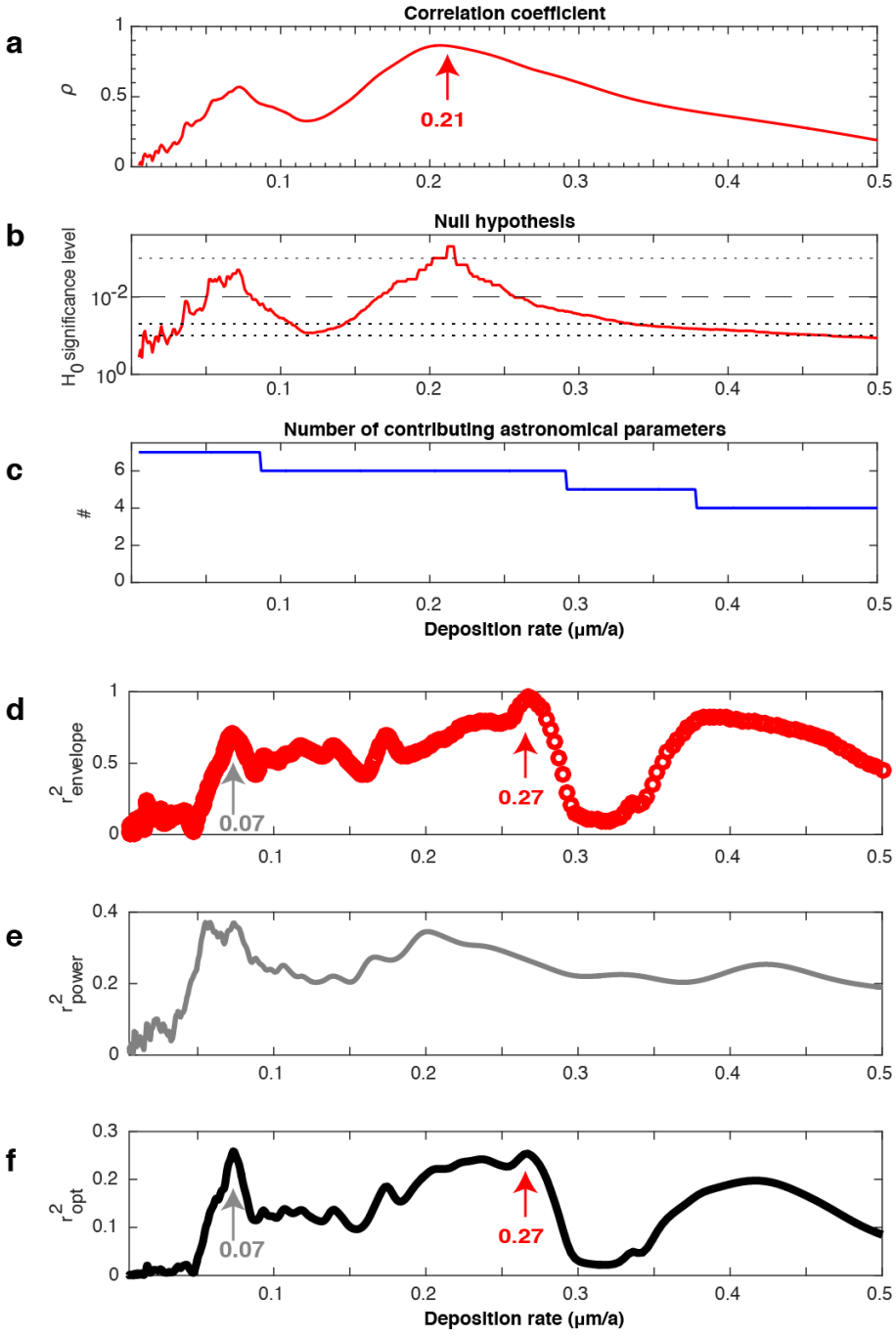

Figure S-12 Sphalerite deposition rate. (**a**) The COCO analysis shows optimal deposition rate at 0.21 µm/a. (**b**) Null hypothesis testing of the data series indicates that 0.07 µm/a and 0.21 µm/a deposition rate have significance levels less than 1 %. Significance levels are estimated using Monte Carlo simulations of 2000 iterations. (**c**) Number of contributing astronomical parameters in the test deposition rate ranging from 0.005 to 0.5 with a step of 0.001 µm/a. (**d**) Squared correlation coefficient for the amplitude envelope fit ($r^2_{envelope}$) indicating the optimal deposition rate of 0.21 µm/a and (**e**) the spectral power fit (r^2_{power}) at test deposition rate. (**f**) Combined envelope and spectral power fit (r^2_{opt}) at test deposition rate.

Supplementary Information References

Anderson, T.C. (2013) Geothermal potential of deep sedimentary basins in the United States. *Energy and Geoscience Institute, Univ. Utah, (www.egi.utah.edu).*

Abràmoff, M.D., Magalhães, P.J., Ram, S.J. (2004) Image processing with *ImageJ*. *Biophotonics international* 11, 36-42.

Barnes, H.L. (2015) Hydrothermal processes. *Geochemical Perspectives* 4, 1-93.

Berger, A., Loutre, M.-F., Dehant, V. (1989) Pre-quaternary Milankovitch frequencies. *Nature* 342, 133.

Bethke, C.M., 1986. Hydrologic constraints on the genesis of the Upper Mississippi Valley mineral district from Illinois basin brines. *Economic Geology* 81, 233-249.

Brannon, J.C., Podosek, F.A., Mclimans, R.K. (1992) Alleghenian age of the Upper Mississippi Valley zinc–lead deposit determined by Rb–Sr dating of sphalerite. *Nature* 356, 509-511.

Kodama, K.P., Hinnov, L. (2015) *Rock Magnetic Cyclostratigraphy*. Wiley-Blackwell.

Lasaga, A.C. (1984) Chemical kinetics of water-rock interactions. *Journal of Geophysical Research: Solid Earth* 89, 4009-4025.

Laskar, J., Robutel, P., Joutel, F., Gastineau, M., Correia, A.C.M., Levrard, B. (2004) A long-term numerical solution for the insolation quantities of the Earth. *Astronomy & Astrophysics* 428, 261-285.

Li, M., Hinnov, L., Kump, L. (2019a) Acycle: Time-series analysis software for paleoclimate research and education. *Computers & Geosciences* 127, 12-22.

Li, M., Huang, C., Ogg, J., Zhang, Y., Hinnov, L., Wu, H., Chen, Z.-Q., Zou, Z. (2019b) Paleoclimate proxies for cyclostratigraphy: Comparative analysis using a Lower Triassic marine section in South China. *Earth-Science Reviews* 189, 125-146.

Li, M., Kump, L.R., Hinnov, L.A., Mann, M.E. (2018) Tracking variable sedimentation rates and astronomical forcing in Phanerozoic paleoclimate proxy series with evolutionary correlation coefficients and hypothesis testing. *Earth and Planetary Science Letters* 501, 165-179.

Mann, M.E., Lees, J.M. (1996) Robust estimation of background noise and signal detection in climatic time series. *Climatic Change* 33, 409-445.

Mclimans, R.K., Barnes, H.L., Ohmoto, H. (1980) Sphalerite stratigraphy of the upper Mississippi Valley zinc-lead district, southwest Wisconsin. *Economic Geology* 75, 351-361.

Meyers, S.R. (2015) The evaluation of eccentricity-related amplitude modulation and bundling in paleoclimate data: An inverse approach for astrochronologic testing and time scale optimization. *Paleoceanography* doi: 10.1002/2015PA002850.

Nelson, P.H., Kibler, J.E. (2003) *A catalog of porosity and permeability from core plugs in siliciclastic rocks*. U.S. Geological Survey, Open-file Report 03-420, 1-7.

Roedder, E. (1968) The non-colloidal origin of 'colloform' textures in sphalerite ores. *Economic Geology* 63, 451-471.

Rowan, E.L., Goldhaber, M.B. (1996) *Fluid inclusions and biomarkers in the Upper Mississippi Valley zinc-lead district: implications for the fluid-flow and thermal history of the Illinois basin*. US Government Printing Office.